Quantum Electronics **40** (4) 349 – 354 (2010)

INTERACTION OF LASER RADIATION WITH MATTER. LASER PLASMA

PACS numbers: 23.35.+g; 52.38.Ph; 52.50.Jm
DOI: 10.1070/QE2010v040n04ABEH014064

Excitation of nuclear isomers by X rays from laser plasma*

A.A. Andreev, K.Yu. Platonov, Yu.V. Rozhdestvenskii, F.F. Karpeshin. M.B. Trzhaskovskaya

***Abstract*. The possibility of obtaining isomer nuclei is studied by the example of the molybdenum isomer ^{93}Mo upon irradiation of a niobium ^{93}Nb target by $\sim$ 50-J, 100-fs laser pulses. It is shown that the modern laser technique allows production of isomer nuclei by accelerated protons and radiative de-excitation of isomer nuclear states by thermal or line X-rays from laser plasma.**

Keywords: *excitation of nuclear isomers, laser acceleration of protons, X rays from plasma.*

1. Introduction

At present, the study of the isomer nucleus excitation and de-excitation with the help of X rays from hot laser plasma attracts significant interest [1]. Investigation of these processes is both of fundamental interest, for example, development of a new approach to nuclear spectroscopy of low-energy transition and of practical interest – possibility of designing a gamma laser and recycling of nuclear waste. Low-energy radiative transitions in isomer nuclei were termed 'anti-Stokes' ones [2]. The theory of radiative processes with their participation was developed for a long time in a number of papers [1 – 6]. However, the experimental papers studying nuclear processes caused by intense X rays are scarce. This is explained, first of all, by the lack of nuclear spectroscopic data on the presence of low-energy (less than 100 keV) transitions in nuclei [7]. As a result, in planning such experiments, scientists mainly have to grope in the dark because even if the data on radiative absorption cross sections, excited-state lifetimes of nuclei for the transition energy below 100 keV are known, they have an insufficient accuracy for performing experiments with the given energy of the X-ray pump quantum. In this case, radiative nuclear processes can be observed by using two experimental schemes. In the first scheme, plasma of the low-energy transition of a stable nucleus is pumped by X rays and then quanta emitted during the reverse transition are observed. In this case, detection of this effect requires rather sophisticated devices of temporal selection of nuclear γ quanta generated from the pump quanta [1]. The second scheme, the so-called two-stage pump scheme [7], involves preparation of a long-lived (isomeric) excited nuclear state and then its excitation by an X-ray quantum up to the first active state whose decay can be observed by using detection of nuclear γ quanta (or other nuclear particles) with the energy differing manifold from the pump quanta energy.

Note that production of nuclear isomers is also possible with the help of a laser accelerator generating intense proton beams [8] and the laser used in such an accelerator allows following de-excitation of the isomer by X rays from hot laser plasma. To this end, in both cases the X-ray pump intensity de-exciting the isomer should be very high because nuclear transitions with the energy below 100keV have high multipolarity degrees and small radiative widths. For these transitions, the use of thermal and linear radiation from laser plasma produced upon irradiation of solid-state targets by intense laser pulses is optimal in observing the effects of nuclear excitation. For example, the intensity of thermal X rays from laser plasma produced upon irradiation of a heavy (Au, Ag) solid-state target by a $10^{17} - 10^{19}$-W cm^{-2} laser pulse can be tens of percent of the laser pulse intensity. The energy of thermal X-ray quanta corresponding to the maximum of Planck's spectrum is several kiloelectronvolts (up to 10 keV), and this plasma at present is a source of X rays with a highest peak intensity. X-ray quanta with a higher energy (up to 100 keV) while retaining the high (of the order of Planck's one) radiation intensity can be obtained also with the help of radiation of K_α lines in laser plasma (the parameters of the lines are given, for example, in [9]).

In this paper, we describe quantitatively the processes of radiative excitation of nuclei by using the modern laser technologies and determine the physical parameters of excitation for which detection of the nuclear processes caused by X rays is reliable. In this case, consideration presented below is suitable for de-excitation of any isomer with a specified structure of nuclear and electron (to take electron conversion into account) levels and concrete numerical estimates are presented for the isomer ^{93}Mo. The advantage of this isomer is the extremely low (0.0361) coefficient of internal electron conversion, significant lifetime of the isomer state ($\sim$ 7 h), and high (268 keV) energy

* Reported at the conference 'Laser Optics 2008', St. Petersburg, Russia.

A.A. Andreev, K.Yu. Platonov, Yu.V. Rozhdestvenskii Institute for Laser Physics, Federal State Unitary Enterprise "Scientific and Industrial Corporation 'S.I. Vavilov State Optical Institute'", Birzhevaya liniya 12, 199034 St. Petersburg, Russia;
e-mail: alex2_andreev@yahoo.com, konstantin_platonov@yahoo.com;
F.F. Karpeshin. M.B. Trzhaskovskaya St. Petersburg State University, Universitetskaya naberezhnaya 7, 199034 St. Petersburg, Russia

Received 28 January 2009; revision received 19 February 2010
Kvantovaya Elektronika **40** (4) 349 – 354 (2010)
Translated by I.A. Ulitkin

of the γ quantum produced during the decay, which makes it possible to separate rather easily the quanta produced during nuclear processes from X-ray pump quanta. At the same time, a disadvantage of this Mo isomer is the absence of the K_α line whose energy is close to the de-excitation energy 4.80 keV. As a result, this molybdenum isomer can be pumped only by X rays from laser plasma.

The database [10] presents the scheme of γ transitions of the ^{93}Mo nucleus (Fig. 1): the isomer state $|1\rangle$ has the energy of 2424.89 keV with the lifetime of 6.85 h, and the excited state $|3\rangle$ – the energy of 2429.69 keV (17/2+) and the lifetime of 3.53 ns. The radiative transition occurs to the level with the energy of 2161.83 keV (the state $|2\rangle$, 13/2+), which then nonradiatively decays. The energy of the produced γ quantum is 267.90 keV upon transition from the $|3\rangle$ level to the $|2\rangle$ level with the transition multipolarity E2. Other nuclear levels of ^{93}Mo are not participating in the selected channel of the isomer state de-excitation. Consider the processes of production and de-excitation of isomer nuclei by high-power laser radiation by the example of ^{93}Mo.

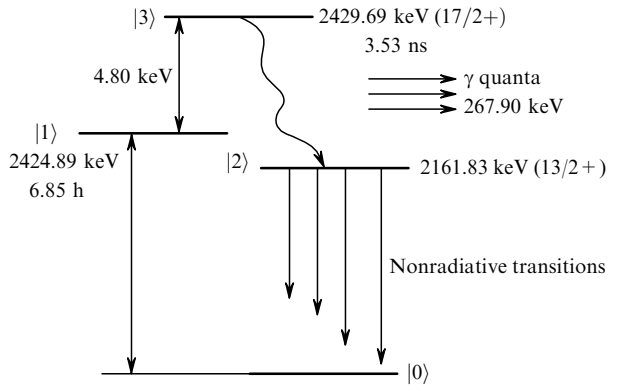

Figure 1. Energy level diagram of low-energy transitions of the ^{93}Mo molybdenum isomer ($|0\rangle$, $|1\rangle$, $|2\rangle$, and $|3\rangle$ are the ground, isomer, final, and active states).

2. Production of an isomer with the help of intense laser radiation

In producing an isomer due to nuclear reaction with the help of an accelerator, isomer states of ^{93}Mo are populated with a probability higher than 0.001 in the reaction ^{93}Nb(p,nγ) with the proton energy starting from 5–6 MeV. These population probabilities are caused by the equilibrium between generation and decay of ^{93}Mo isomer nuclei upon continuous irradiation of a niobium (^{93}Nb) target by protons.

Consider the possibility of producing an isomer with the help of a super-high-power laser operating as an accelerator. In this case, the number of Mo isomer nuclei produced during the action of a separate laser pulse can be estimated as $N_{\mathrm{Mo}} = N_{\mathrm{p}} n_{\mathrm{Nb}} \sigma_{\mathrm{Nb}} l_{\mathrm{p}}$, where the free path length l_{p} of a proton with the energy ~ 5 MEv in metallic niobium with the concentration $n_{\mathrm{Nb}} \approx 6 \times 10^{22}$ cm^{-3} calculated by using the SRIM software [11] is equal to ~ 100 μm. The cross section σ_{Nb} of the reaction ^{93}Nb(p, nγ) is $\sim 10^{-26}$ cm^2, and $10^{12} - 10^{13}$ protons can be produced per one laser pulse [8]. Then, the upper estimate of the number of ^{93}Mo isomer nuclei produced during the action of a single laser pulse with the parameters stated above is $\sim 6 \times 10^7$. At the same time, protons with the maximum energy are generated on an area of the order of the laser spot area, $S_{\mathrm{L}} \approx 10^{-5}$ cm^2, and the volume $S_{\mathrm{L}} l_{\mathrm{p}}$ contains $\sim 6 \times 10^{15}$ niobium nuclei. As a result, $\sim 10^4$ laser pulses are required so that the number of ^{93}Mo isomer nuclei constitute 0.1% of the number of ^{93}Nb niobium nuclei, these pulses being shot during the time smaller than the isomer lifetime (~ 7 h). Therefore, the pulse repetition rate in this case is 0.4 Hz, which is quite feasible for modern laser technologies.

Thus, it is possible to obtain the ^{93}Mo isomer nuclei concentration of $\sim 10^{19}$ cm^{-3} with the help of a ~ 50-J, 100-fs laser with a pulse repetition rate of ~ 1 Hz, intensity of 5×10^{19} W cm^{-2} and laser spot area of 10^{-5} cm^2. With this method of isomer production, a continuously advancing polystyrene ribbon (or a rotating disk) whose protons are incident on the Nb target can serve as a laser target for proton generation.

3. Generation of X rays to pump an isomer

Papers [4, 5] describe the computational method, which makes it possible to calculate the conversion coefficient of laser radiation energy into X-ray pump energy of a nuclear isomer. When an isomer target is pumped by thermal X rays from laser plasma, the nuclear line width Γ_3 (the level width is $|3\rangle$) is determined by the Doppler effect: $\Gamma_3 \sim \Gamma_{3\mathrm{D}} = \omega_{\mathrm{x}} v_{\mathrm{Ti}}/c$, where ω_{x} is the X-ray quantum frequency and v_{Ti} is the thermal velocity of a plasma ion. Figure 2 shows the conversion coefficient ε_T of the laser radiation energy into the thermal X-ray energy falling into the spectral region of the nuclear pump for a molybdenum target as a function of the laser radiation intensity. The laser pulse duration was taken equal to 200 ps. The target thickness, corresponding to Fig. 2, should exceed ~ 40 μm (the absorption length of a quantum with the energy 4.8 keV in molybdenum, according to data from [9]) to provide a sufficient optical thickness and Planck's spectrum of X-ray quanta. Using a 20-J, 200-ps laser pulse with the

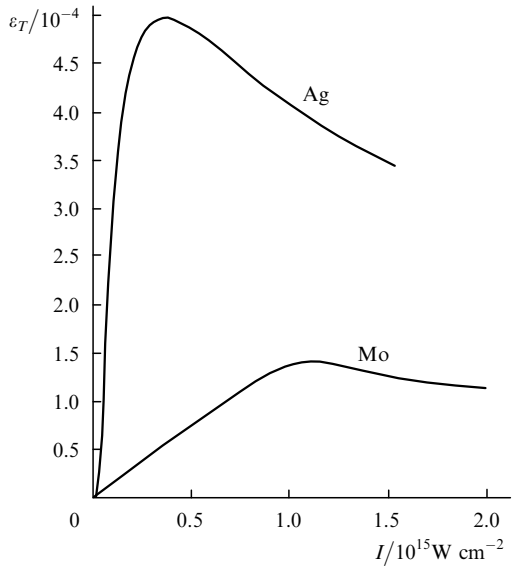

Figure 2. Conversion coefficient of the laser radiation energy into the thermal X-ray energy as a function of the laser radiation intensity for a molybdenum or silver target.

focal spot diameter of 100 μm, it is possible to obtain the optimal laser radiation intensity $\sim 1.3 \times 10^{15}$ W cm^{-2}. In this case, the maximal conversion coefficient is 1.5×10^{-4}, which corresponds to the number of pump quanta falling into the spectral region conforming to the Doppler broadened nuclear level, $N_x = \varepsilon_T(20\ \text{J}/4.8\ \text{keV}) \approx 4 \times 10^{12}$.

Consider another method for generating X-ray pump (see Fig. 2 from paper [4]), which is realised by focusing laser radiation on an outside silver target. The choice of the material of the additional target arises from the fact that silver and molybdenum have close nuclear charges (47 and 42) and masses (107 and 93). Then, the additional target should be located at a distance L_t from the isomer target that is longer than the ion path length during the laser pulse action t_L: $L_t \geqslant c_s t_L \approx 20$ μm (c_s is the ion sound velocity), and the isomer target should be bent and overlap as far as possibly the large solid angle in order to avoid geometric pump-radiation losses. Figure 2 presents the results of calculation of the conversion coefficient for a silver target. One can see that the conversion coefficient in this case is approximately three times higher than that for the molybdenum target; however, the geometrical losses are substantial in this case and are approximately of the same order. As a result, the advantage of the outside target is lower heating and absence of the spread of the isomer material. The Doppler width of the nuclear level for this target is much smaller and comparable with the natural width of the excited isomer level: $(3.53\ \text{ns})^{-1}$.

The modern level of the development of laser technologies makes it possible to produce laser plasma with a temperature of several kiloelectronvolts. According to this, isomer nuclear levels with energies not exceeding 10 keV can be excited by thermal X rays. Use of laser plasma to excite K_α lines makes it possible to increase by an order of magnitude the pump quantum energy of nuclear isomers but requires coincidence of the K_α transition energy with the isomer transition energy, which is a rare case [3].

4. Estimation of the number of isomer nuclei de-excited by thermal X rays from laser plasma

Let us estimate the number of excited nuclei upon irradiation of a nuclear isomer, whose energy level diagram is shown in Fig. 3, by X rays from laser plasma. Thermal X rays from laser plasma pump the $|1\rangle - |3\rangle$ low-energy transition of the nuclear isomer. As a result, a part of isomer nuclei during the time τ of plasma emission undergo transition to the $|3\rangle$ state, followed by the spontaneous decay into the low-lying state $|2\rangle$, which leads to emission of γ quanta with the energy corresponding to the $|3\rangle - |2\rangle$ transition.

Isomer nuclei from the $|3\rangle$ state can both decay into the $|2\rangle$ state and undergo transition to the $|1\rangle$ state emitting an X-ray quantum $\hbar\omega$, or due to the electron conversion there occurs a nonradiaitve transition to the state shown in Fig. 3 as $|4\rangle$. The probabilities of the mentioned transitions are proportional to radiation widths of nuclear levels and the electron conversion coefficients. In particular, the extremely low (0.0361) coefficient of internal electron conversion makes the $|1\rangle - |4\rangle$ transitions unlikely for the Mo isomer. Let us pass to a detailed description of the processes of excitation and decay of nuclear levels.

The transition probability w_{13} of a nucleus from the $|1\rangle$ isomer state to the $|3\rangle$ excited state during the time τ of the

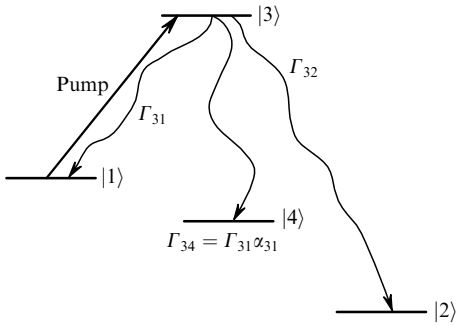

Figure 3. Energy level diagram of excitation of the nuclear isomer: $|1\rangle$ is the isomer state; $|3\rangle$ is the active state of the nuclear isomer; $|2\rangle$, $|4\rangle$ are the final states to which a nuclear isomer undergoes transition after emission of γ quanta or due to internal conversion.

X-ray pump (in the order of the laser pulse duration) is determined by the perturbation theory (Fermi rule) as

$$w_{13} = \tau \frac{2\pi}{\hbar} |\langle 3|\hat{V}|1\rangle|^2 \delta(\varepsilon_3 - \varepsilon_1 - \hbar\omega), \tag{1}$$

where $\hat{V}$ is the operator of nucleus–electromagnetic-field interaction; ε_1 and ε_2 are the energies of $|1\rangle$ and $|3\rangle$ levels.

In the case of magnetic dipole transitions with the multipolarity M1, the operator $\hat{V}_{M1}$ of interaction with the external field H can be written in the form

$$\hat{V}_{M1} \sim \mu_p H \hat{s}, \tag{2}$$

where $\mu_p = e\hbar/(m_p c)$ is the nuclear magnetic moment corresponding to the proton mass m_p; $\hat{s}$ is the spin operator of a nucleus. For a transition with the multipolarity E3, the operator $\hat{V}_{E2}$ of interaction with the external field E can be presented in the form [12]

$$\hat{V}_{E2} = Q_{\alpha\beta} \frac{\partial E_\alpha}{\partial r_\beta}, \tag{3}$$

where $Q_{\alpha\beta}$ is the nuclear quadrupole tensor whose components are approximately equal to er_{nuc}^2; $\alpha, \beta = x, y, z$; $r_{nuc} \sim 10^{-13} A^{1/3}$ is the characteristic size (in centimetres) of a nucleus with the mass A. The matrix element $\langle 3|\hat{V}|1\rangle$ is estimated in this case as $eE\omega r_{nuc}^2/c$. When taking into account the finite width Γ_3 of the upper excited level, the δ-function in (1) is replaced by the asymptotic representation:

$$\delta(\varepsilon_3 - \varepsilon_1 - \hbar\omega) \approx \frac{\hbar\Gamma_3/2\pi}{(\varepsilon_3 - \varepsilon_1 - \hbar\omega)^2 + (\hbar\Gamma_3/2)^2}. \tag{4}$$

In the expression for the matrix element $|V_{13}|^2$, it is convenient to separate the Poynting vector for the pump wave $cH^2/(4\pi)$ or $cE^2/(4\pi)$, and to express the remaining part, corresponding to the magnetic or quadrupole moment, by the radiation widths of nuclear transitions [12]

$$\Gamma_{31}^{M1} = \frac{4\omega^3 |\mu_p s_{13}|^2}{3c^3\hbar}, \quad \Gamma_{31}^{E2} = \frac{\omega^5 |Q_{13}|^2}{15c^5\hbar}. \tag{5}$$

Note that paper [13] presents expressions for the widths $\hbar\Gamma_{31}^{M1} = 2.1 \times 10^{-14}(\hbar\omega)^3$, $\hbar\Gamma_{31}^{E2} = 4.9 \times 10^{-26}(\hbar\omega)^5 A^{4/3}$, where $\hbar\Gamma_{31}^{M1}$, $\hbar\Gamma_{31}^{E2}$, and $\hbar\omega$ should be in kiloelectronvolts.

However, these expressions do not take into account the specific character of a concrete nucleus, and they can yield the radiation widths of nuclear levels, which differ from tabulated data. Here, the effect of the electron conversion changing the nuclear radiation widths by several orders of magnitude is not taken into account [14].

As a result, expression (1) for the $|1\rangle - |3\rangle$ transition probability of the nuclear isomer (E2 in the case of ^{93}Mo) can be written via the cross section σ_x of the radiation absorption of the pump quanta and the flux (in s^{-1} cm^{-2}) of monochromatic pump quanta $I_x = cE^2/(4\pi\hbar\omega)$:

$$w_{13} = \tau I_x \sigma_x, \tag{6}$$

where τI_x is the total number N_x of pump quanta per unit area of the isomer target, and

$$\sigma_x = \frac{60\pi c^2}{\omega^2} \frac{\hbar^2 \Gamma_{31}^{E2} \Gamma_3}{(\varepsilon_3 - \varepsilon_1 - \hbar\omega)^2 + (\hbar\Gamma_3/2)^2}. \tag{7}$$

Note that in the case of resonance ($\hbar\omega = \varepsilon_3 - \varepsilon_1$), the maximal cross section $\sigma_{x\max} = 15\lambda_x^2 \Gamma_{31}^{E2}/(\pi\Gamma_3)$. In the case of magnetic dipole transitions, Γ_{31}^{M1} is used instead of the width Γ_{31}^{E2} in (7), and the numerical coefficient will be equal to 3π instead of 60π.

In the case of the thermal X-ray pump with a continuous spectrum, the flux (in s^{-1} cm^{-2}) of the pump quanta will be determined by the Planck distribution: $dI_x = \omega^2 d\omega \times \{\pi^2 c^2 [\exp(\hbar\omega/T_e) - 1]\}^{-1}$, where T_e is the electron temperature. To calculate the excitation probability in (6), it is necessary to perform integration over the entire Planck spectrum of the X-ray pump quanta:

$$w_{13} = \frac{\tau}{\pi^2 c^2} \int_0^\infty \frac{\omega^2}{\exp(\hbar\omega/T) - 1} \sigma_x(\omega) d\omega. \tag{8}$$

Because of the sharp dependence of cross section (7) on the pump quantum energy, the integral in (8) is easily calculated, and the number N_3 of nuclei excited from the $|1\rangle$ isomer state to the $|3\rangle$ active state, in the case of resonance excitation by X-ray quanta, can be written in the form [4]

$$N_3 = 120 N_{10} \frac{2J_3 + 1}{2J_1 + 1} \frac{\Gamma_{31}}{\Gamma_3} \Gamma_3 \tau \left[\exp\left(\frac{\varepsilon_3 - \varepsilon_1}{T_e} \right) - 1 \right]^{-1}, \tag{9}$$

where N_{10} is the initial number of isomer nuclei in the $|1\rangle$ state irradiated by the pump quanta; Γ_{31}, depending on the transition, is determined by expression (5). These isomers reside in the cylindrical region with the base area in the order of the laser spot area S_L and the height in the order of the absorption length l_x of the X-ray quantum (it is assumed that the laser spot diameter is larger than the absorption length). In estimating N_{10}, it is necessary to take into account that the limiting concentration of the molybdenum isomer in the solid-state target can achieve 10^{-3} of the total concentration of nuclei. In expression (9), the total width Γ_3 of the $|3\rangle$ excited state is not specially reduced in order to point out that the number of excited nuclei is formally independent of this parameter, and the Doppler broadening of the nuclear line does not lead to an increase in the number of excited nuclei, which differs from the results of paper [6]. Expression (9) describes the initial stage of the excitation process when the number of the active nuclei is proportional to the pump duration τ. The finite pump duration is limited by the lifetime τ_3 of the $|3\rangle$ excited state ($\tau_3 = 3.53$ ns for Mo) because at large τ a dynamic equilibrium between excitation and decay of the $|3\rangle$ state is established. Expression (9) additionally takes into account different statistical weights of the initial and final nuclear states by introducing $J_{1,3}$ spins of these states.

Consider now generation of the γ quantum during the decay of the $|3\rangle$ state, which after excitation can decay both in the states $|1\rangle$ and $|2\rangle$ and in the state $|4\rangle$ responsible for the electron conversion of the emitted quanta. The lifetime τ_3 of the $|3\rangle$ excited state is estimated by the expression

$$\tau_3^{-1} = \Gamma_{31}(1 + \alpha_{31}) + \Gamma_{32}(1 + \alpha_{32}), \tag{10}$$

where α_{31}, α_{32} are the internal conversion coefficients for the transitions $|3\rangle - |1\rangle$ and $|3\rangle - |2\rangle$, respectively; and $\Gamma_{31,32}$ are the radiation transition widths. The probability that a hard γ quantum will be generated during the decay of the $|3\rangle$ state, will be equal to the product $\tau_3\Gamma_{32}$ (the absorption probability of this quantum by the electron shell is $\tau_3\alpha_{32}\Gamma_{32}$).

The total number N_γ of γ quanta produced during the emission of the laser plasma is found by multiplying the number of excited nuclei (9) by the generation probability of a γ quantum [5]:

$$N_\gamma = N_3 \Gamma_{32} \tau_3 \approx 10^2 N_{10} \frac{2J_3 + 1}{2J_1 + 1} \Gamma_{31} \Gamma_{32} \tau \tau_3 \times \left[\exp\left(\frac{\varepsilon_3 - \varepsilon_1}{T_e} \right) - 1 \right]^{-1}. \tag{11}$$

Note again that expression (11) cannot be used in the saturation regime of nuclear levels and describes only the initial stage of the de-excitation process when the quantum yield is proportional to the pump duration τ. In (11), the limiting pump duration is $\tau \sim \tau_3$. Expression (11) makes it possible to evaluate the possibility (criterion $N_\gamma > 1$) of radiative de-excitation of the isomer nuclear state with the specified structure of nuclear and electron (to take conversion into account) levels by thermal X rays.

Let us estimate now the number of emitted γ quanta in the case of the ^{93}Mo isomer by setting the laser plasma temperature such that the energy of the X-ray pump quantum at the $|1\rangle - |3\rangle$ transition corresponds to the maximum of the Planck distribution [$(\varepsilon_3 - \varepsilon_1)/T_e \approx 2.8$]:

$$N_\gamma \approx 10 N_{10} \Gamma_{31} \Gamma_{32} \tau \tau_3. \tag{12}$$

The internal conversion coefficients in (10) are calculated with the help of the RAINE software package [14]: $\alpha_{31} \approx 4.87 \times 10^5$, $\alpha_{32} = 0.03$. The low α_{32} is caused by the fact that the $|3\rangle - |2\rangle$ transition in the case of the molybdenum isomer has the energy 268 keV, and the $|3\rangle - |1\rangle$ transition is a low-energy transition with the energy 4.8 keV (see Fig. 1). Therefore, hard quanta with the energy 268 keV do not fit into the range of characteristic energies of the electron shell. The excited-state lifetime of the Mo isomer, taking into account the coefficients of internal conversion and radiation widths is determined only by the radiation width of the $|3\rangle - |2\rangle$ transition. Because τ_3 is known from reference data and the ratio of the partial widths is $\Gamma_{31}/\Gamma_{32} \approx (4.8/268)^5$ (both transitions have the multipolarity E2), we, knowing that $\Gamma_{32} \sim \tau_3^{-1} = 3 \times 10^8$ Hz, can

obtain $\Gamma_{31} \approx 0.5$ Hz. Thus, all the quantities in expression (12) are found.

Note that the internal electron conversion at the $|1\rangle - |3\rangle$ transition can hamper generation of hard nuclear quanta under condition $\alpha_{31}\Gamma_{13} > \Gamma_{32}$, which is not fulfilled for ^{93}Mo.

As a result of the performed estimations at $\tau \sim 0.1$ ns ($\tau \ll \tau_3$), the number of emitted γ quanta (12) is

$$N_\gamma = 2 \times 10^{-10} N_{10}. \tag{13}$$

Then, to obtain, for example, $N_\gamma \sim 10^2$, it is necessary to have $N_{10} \sim 10^{12}$ in the pump region, which corresponds to the total number of isomer nuclei in the laser spot region of diameter $100\lambda_L \sim 10^{-2}$ cm. In this case, we assumed that pump radiation is absorbed in the $40\lambda_L$-thick layer with the molybdenum isomer concentration in the laser target equal to 10^{-3} of the solid-state target.

Therefore, the estimate of the possibility of de-exciting the isomer states requires detailed information on the structure and radiation widths of nuclear levels and the knowledge of the electron conversion coefficients of nuclear transitions. Then, the method presented in this section makes it possible to consider other isomer nuclei.

Note that the obtained estimate of the number of emitted γ quanta (13) is valid for such pump durations at which the population of the $|3\rangle$ level is small. A more rigorous analysis requires using, instead of the transition probability (1), nonstationary equations for the populations of all the nuclear levels participating in the de-excitation.

5. Population dynamics of nuclear levels during de-excitation of the isomer state by pulsed X rays

Consider now the nonstationary model of the isomer nucleus excitation by X rays from laser plasma to produce γ quanta with the energy corresponding to the $|3\rangle - |2\rangle$ transition. The equations for the density matrix elements of the system of nuclear levels can be written as the equations for the populations $N_1 - N_4$ of the corresponding states:

$$\frac{dN_1}{dt} = W(t)s_{13} + \gamma_{13}N_3, \quad \frac{dN_2}{dt} = \gamma_{23}N_3,$$
$$\frac{dN_3}{dt} = -W(t)s_{13} - 2N_3, \quad \frac{dN_4}{dt} = \gamma_{43}N_3, \tag{14}$$

and the equation for the nondiagonal matrix elements s_{13} of the $|1\rangle - |3\rangle$ transition has the form

$$\frac{ds_{13}}{dt} = -2W(t)(N_1 - N_3) - s_{13}. \tag{15}$$

In equations (14), (15), time t is measured in the units of τ_3; the X-ray pump intensity has a Gaussian time profile $W(t) = G\exp[-(t-\tau_0)/\tau_p)^2]$ with the characteristic pump duration τ_p and the instant of the pump 'switching on' $t = \tau_0$; the dimensionless matrix element is $G = \langle 3|\hat{V}|1\rangle\tau_3/\hbar$ ($\langle 3|\hat{V}|1\rangle$ was estimated in the previous section); $\gamma_{13} = \Gamma_{31}\tau_3$; $\gamma_{23} = \Gamma_{32}\tau_3$; $\gamma_{43} = \Gamma_{31}\alpha_{31}\tau_3$. Expression (1) is the solution of equations (14), (15) at $t \to 0$ and is independent of the pump intensity duration, i.e. represents an expansion in the Taylor series of a more general solution of the nonstationary system.

Figure 4 presents the results of numerical solution of system (14), (15), which explicitly demonstrate that the population of the $|2\rangle$ state is determined by the dimensionless matrix element G (with respect to the pump intensity) and τ_p (with respect to the pump duration). At $\tau_p < 1$, the population of the $|2\rangle$ state increases linearly with increasing τ_p, as was shown in the previous section. In addition, one can see from Fig. 4 that the population of the $|2\rangle$ state becomes noticeably other than zero if $G \gtrsim 0.1$ (i.e. $\langle 3|\hat{V}|1\rangle \sim 0.1\hbar/\tau_3$) and $\tau_p \geqslant 0.1$.

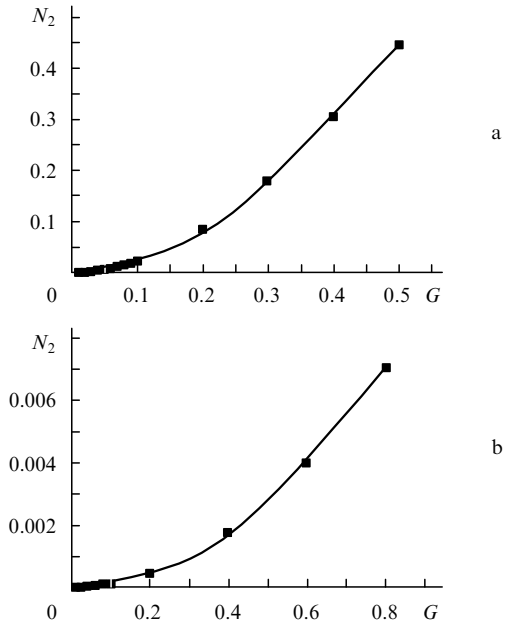

Figure 4. Dependence of the $|2\rangle$ state population N_2 on the dimensionless pump intensity G at $\gamma_{13} = 10^{-8}$, $\gamma_{23} \sim 1$, $\gamma_{43} = 10^{-5}$, $\tau_p = 1$ (a) and 0.1 (b).

Figure 5 presents the temporal dynamics of nuclear level populations for $\tau_p = 1$, $G = 0.5$, and $\tau_0/\tau_p = 6$. One can see that in the initial time interval $t \in [6; 6.5]$ the populations of all the levels change linearly with time, in accordance with the expressions of the previous section. At $7 \geqslant t \geqslant 6.5$ the population of the $|3\rangle$ upper level normalised to unity is saturated at the level ~ 0.2, while the populations of the levels $|1\rangle$, $|2\rangle$ continue to change linearly with time. At $t \geqslant 7$, the pump terminates and the population of the $|3\rangle$ upper

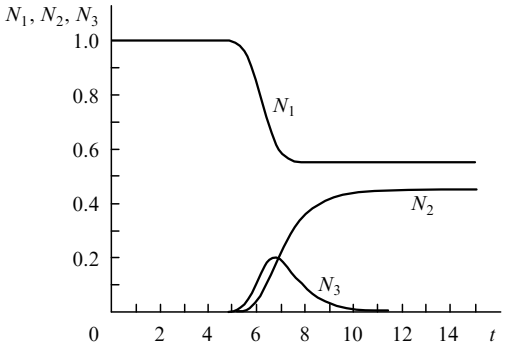

Figure 5. Temporal population dynamics N_1, N_2 and N_3 of the levels $|1\rangle$, $|2\rangle$, and $|3\rangle$ at $\tau_p = 1$, $G = 0.5$, and $\tau_0/\tau_p = 6$.

level starts decreasing, while the populations of levels $|1\rangle$, $|2\rangle$ tend to constant values, excitation of the isomer state (change in the population of the $|1\rangle$ level) terminates earlier than emission of the excited state (change in the population of the $|3\rangle$ level). At the given pump duration and intensity, ~ 0.4 of the total number of isomer nuclei irradiated by the pump decay.

For the ^{93}Mo, we will estimate numerically the pump intensity at which the dimensionless matrix element G achieves the value of ~ 0.1. It follows from expression (3) and definition of G that the dimensionless electric field strength [$\tilde{E} = eE/(m_e c\omega_L)$, where m_e is the electron mass and ω_L is the optical laser frequency] of the X-ray pump is

$$\tilde{E} \sim 0.1 \frac{\hbar}{r_{nuc}^2 \omega_x \omega_L m_e \tau_3}. \quad (16)$$

At the energy $\hbar\omega_x = 4.8$ keV and wavelength $\lambda_L = 2\pi c \times \omega_L^{-1} = 1$ μm, expression (16) yields $\tilde{E} \approx 0.3$. At such field strengths the X-ray pump intensity is $\sim 10^{17}$ W cm^{-2}. By equating the pump intensity to the flux density of Planck's radiation, $cE^2/(4\pi) \sim \sigma T^4$, we obtain the radiation temperature ~ 1 keV required to pump efficiently the Mo isomer. In this case, the pump duration should exceed ~ 0.3 ns ($\tau_p \geqslant 0.1$). For the laser plasma spot area 4×10^{-6} cm^2, the total X-ray pump energy (in the entire Planck spectrum) should be 80 J and the laser pulse energy should be equal to 500 – 1000 J, depending on the conversion coefficient ε_T. These parameters are quite feasible for modern laser technologies.

Therefore, a more rigorous consideration of the population dynamics of the ^{93}Mo nuclear levels during de-excitation of the isomer state by a thermal X-ray pulse also allows one to come to the conclusion that experimental realisation of this process is possible under laboratory conditions.

6. Conclusions

The present level of the development of the laser technique allows efficient investigation of nuclear processes with the help of high-power lasers. In particular, with the laser acceleration of protons it is possible to obtain ^{93}Mo isomer nuclei in a metallic niobium sample as a result of the reaction ^{93}Nb(p, nγ) when a 50-J, $\sim$ 100-fs laser with the pulse repetition rate of several hertz and the laser spot area of 10^{-5} cm^2 is used to generate protons.

High-power lasers can also de-excite nuclear isomer state by the thermal X-ray pump or linear X-ray pump from laser plasma. For example, thermal X rays, obtained upon irradiating a silver target by a 1-kJ, 300-ps laser pulse with the focal spot diameter of 20 μm, are sufficient for de-excitation of ^{93}Mo. In this case, the number of 268-keV hard nuclear quanta emitted during de-excitation is no less than 10^2, which is sufficient to detect the effect.

Consideration of the population dynamics of the nuclear levels has shown that the optimal X-ray pump duration of the laser transition should be in the order of the lifetime τ_3 of the upper excited nuclear level. Because the X-ray emission duration of laser plasma exceeds the laser pulse duration by two – three times, the latter should be two – three times smaller than the lifetime of the excited nuclear level.

Acknowledgements. The authors thank S.G. Garanin and N.V. Zhidkov for the support of the present work.

References

1. Andreev A.V., Volkov R.V., Gordienko V.M., et al. *Zh. Eksp. Teor. Fiz.*, **118**, 1343 (2000) [*JETP*, **91**, 1163 (2000)]; Collins C.B. et al. *Phys. Rev. C*, **37**, 2267 (1988).
2. Eliezer S., Martinez-Val J.M., Paiss Y., Velarde G. *Kvantovaya Electron.* **22**, 1140 (1995) [*Quantum Electron.*, **25**, 1106 (1995)].
3. Letokhov V.S. *Kvantovaya Electron.*, No. 4 (16), 125 (1973) [*Sov. J. Quantum Electron.*, **3** (4), 360 (1973)].
4. Andreev A.V., Platonov K.Yu., Rozhdestvenskii Yu.V. *Zh. Eksp. Teor. Fiz.* **121**, 1002 (2002) [*JETP*, **94**, 862 (2002)].
5. Olariu S., Olariu A. *Phys. Rev. C*, **58** (1), 333 (1998).
6. Afonin V.I. *Fiz. Plazmy*, **35**, 174 (2009).
7. Balwin C.C., Solem J.C. *Rev. Mod. Phys.*, **69**, 1085 (1997).
8. Robson L., Simpson P.T., Clarke R.J., Ledingham K.W.D., Lindau F., Lundh O., McCanny T., Mora P., Neely D., Wahlström C.-G., Zepf M., McKenna P. *Nat. Phys.*, **3**, 58 (2007).
9. http://www-cxro.lbl.gov.
10. http://www.nndc.bnl.gov/ http://ie.lbl.gov/ensdf/.
11. www.srim.org.
12. Berestetskii V.B., Lifshits E.M., Pitaevskii L.P. *Quantum Electrodynamics* (Oxford: Butterworth-Heinemann, 1999; Moscow: Nauka, 1980).
13. Blanc D. Noyaux, particules. *Reacteurs nucléaires* (Paris: Masson, 1987; Moscow: Mir, 1989).
14. Band I.M., Listengarten M.A., Trzhaskovskaya M.B., Fomichev V.I. Preprint Leningrad Inst. Yad. Fiz. No. 289 (Leningrad, 1976), Nos 298–300 (Leningrad, 1977), No. 498 (Leningrad, 1979), and No. 1479 (Leningrad, 1989).